Prediction of solitary ≤3-cm small adrenal metastasis based on ^{18}F-FDG PET/CT using a support vector machine model in lung cancer

LIN ZHAO[1*], HAIFENG CAI[2*], JINGWU LI[3*], WENZHE ZHAO[3], YONGLIANG LIU[4] and LIXIU CAO[3,5]

[1]Department of Computed Tomography, Tangshan People's Hospital, Tangshan, Hebei 063000, P.R. China; [2]Department of Breast Surgery, Tangshan People's Hospital, Tangshan, Hebei 063000, P.R. China; [3]Hebei Key Laboratory of Molecular Oncology, Tangshan People's Hospital, Tangshan, Hebei 063000, P.R. China; [4]Department of Neurosurgery, Tangshan People's Hospital, Tangshan, Hebei 063000, P.R. China; [5]Department of Nuclear Medicine Imaging, Tangshan People's Hospital, Tangshan, Hebei 063000, P.R. China

Received May 14, 2025; Accepted October 17, 2025

DOI: 10.3892/ol.2025.15395

Abstract. The purpose of the present study was to develop a simplified scoring system based on the support vector machine (SVM) classification method to improve the diagnostic performance of ^{18}F-fluorodeoxyglucose (FDG) positron emission tomography/computed tomography (PET/CT) in differentiating solitary small (≤3 cm) adrenal metastases from benign lesions in patients with lung cancer. A total of 197 patients with histopathologically confirmed diagnoses of lung cancer were retrospectively included. All patients had solitary adrenal lesions (long diameter ≤3 cm) showing hyperattenuating features (unenhanced CT values ≥10 HU) on pre-treatment ^{18}F-FDG PET/CT scans. The cohort included 128 cases of metastases and 69 cases of benign lesions. SVM models were developed using five adrenal lesion features and one primary lung cancer feature. Model performance was evaluated by comparing the area under the receiver operating characteristic curve (AUC) and accuracy across eight candidate models. The optimal model was further simplified based on feature weights and value distributions to enhance clinical applicability. The best-performing SVM model demonstrated maximum, minimum and mean accuracies of 98.0% (95% CI, 93.9-100%), 71.4% (95% CI, 57.1-83.7%) and 84.3% (95% CI, 69.4-91.8%), respectively, with corresponding AUC values of 1.000, 0.770 and 0.913, respectively. The simplified scoring system stratified adrenal lesions into three diagnostic categories: Scores <5, benign; scores >6.5, metastatic; and scores 5-6.5, suspicious for metastasis. In conclusion, the present study developed an SVM-based model using ^{18}F-FDG PET/CT imaging features to differentiate solitary small adrenal metastases in patients with lung cancer. The maximum standardized uptake value of the adrenal lesions was the predominant predictive feature. After simplification, the model was converted into a clinically practical scoring system, which may assist clinicians in streamlining clinical staging decisions for patients with lung cancer.

Correspondence to: Dr Lixiu Cao, Department of Nuclear Medicine Imaging, Tangshan People's Hospital, 65 Shengli Road, Lunan, Tangshan, Hebei 063000, P.R. China
E-mail: caolixiu19860301@126.com

Professor Yongliang Liu, Department of Neurosurgery, Tangshan People's Hospital, 65 Shengli Road, Lunan, Tangshan, Hebei 063000, P.R. China
E-mail: liuyongliang1974@126.com

*Contributed equally

Abbreviations: AUC, area under the receiver operating characteristic curve; FDG, fluorodeoxyglucose; KNN, k-nearest neighbor; LD, long diameter; PET/CT, positron emission tomography/computed tomography; ROI, region of interest; SVM, support vector machine; SD, short diameter; SUV_{max}, maximum standardized uptake value; $SUR_{adrenal/liver}$, adrenal-to-liver SUV_{max} ratio; $SUR_{lung/liver}$, lung-to-liver SUV_{max} ratio

Key words: PET/CT, lung cancer, adrenal metastases, SVM

Introduction

Lung cancer persists as the leading cause of cancer-related mortality in men and ranks second in women worldwide (1). Notably, ~70% of lung cancer cases are diagnosed at advanced stages with metastatic dissemination (2). The adrenal glands constitute a frequent metastatic site in this population, with reported incidence rates ranging from 18 to 42% across studies. Notably, 2-4% of these patients present with isolated adrenal metastases that may be amenable to curative interventions (3-5). Emerging evidence has demonstrated that aggressive local therapies, including surgical resection and stereotactic ablative radiotherapy, can markedly improve survival outcomes in patients with solitary adrenal metastases (6,7). These findings underscore the critical need for accurate restaging of solitary adrenal masses in lung cancer management.

Nevertheless, differentiating metastatic lesions from benign adrenal lesions in patients with lung cancer remains clinically challenging (8), particularly for small lesions [long diameter (LD) ≤3 cm] with hyperattenuating features [unenhanced

computed tomography (CT) values ≥10 HU] (9-11). Although conventional imaging modalities offer diagnostic parameters such as CT attenuation values, delayed contrast-enhanced CT patterns and magnetic resonance imaging (MRI) chemical-shift characteristics (12-14), their clinical application faces three major limitations. First, lesion-specific diagnostic thresholds may lack generalizability due to heterogeneous tumor biology. Second, concurrent primary lung malignancies can complicate radiological interpretation. Third, practical challenges exist, including increased radiation exposure from multiphase CT protocols, time-consuming MRI acquisitions that disrupt clinical workflows and contraindications that compromise image quality (such as motion artifacts or metallic implants) (15,16).

^{18}F-Fluorodeoxyglucose (FDG) positron emission tomography (PET)/CT is an imaging modality that provides both anatomical and metabolic information by assessing glucose uptake. This technique has emerged as a reliable non-invasive tool for evaluating adrenal masses (17,18). However, its diagnostic accuracy is limited by two key factors: i) Some benign adrenal lesions (for example, functional adenomas) exhibit increased FDG uptake, potentially leading to Tumor-Node-Metastasis stage overestimation (19,20); and ii) certain adrenal metastases in patients with lung cancer may remain undetected due to low FDG avidity (21). Additionally, previous studies have primarily focused on individual metabolic parameters for differentiating adrenal tumors (22,23), while comprehensive PET/CT-based analyses of solitary small hyperattenuating adrenal lesions in patients with lung cancer remain scarce.

Support vector machine (SVM), a supervised machine learning algorithm, is particularly effective for classification tasks with limited sample sizes. SVM constructs an optimal decision boundary by maximizing the margin between two classes in the training dataset, thereby improving model generalizability (24). SVM has shown promise in classifying solitary pulmonary nodules and lymph nodes (25,26); however, its application to solitary small hyperattenuating adrenal lesions in lung cancer remains unexplored.

To address these gaps in the knowledge, the present study aimed to develop an interpretable SVM-based classification model to enhance the diagnostic accuracy of ^{18}F-FDG PET/CT in distinguishing between metastatic and benign solitary small hyperattenuating adrenal lesions in patients with lung cancer.

Patients and methods

Patients. Patients treated in Tangshan People's Hospital (Tangshan, China) between October 2022 and October 2024 were retrospectively included in the present study if they met the following criteria: i) Histopathologically confirmed lung cancer prior to ^{18}F-FDG PET/CT examination; and ii) the presence of a solitary small (LD ≤3 cm) hyperattenuating (unenhanced CT value ≥10 HU) adrenal lesion. The current study was approved by the Institutional Ethics Committee of Tangshan People's Hospital (approval no. RMYY-LLKS-2023202). The requirement for written informed consent was waived due to the retrospective nature of the study. The diagnostic criteria for adrenal metastases were as follows: i) Histopathological confirmation; or ii) interval development of an adrenal mass on follow-up CT (compared with a prior scan showing normal adrenal glands); or iii) short-term interval growth [defined as a ≥20% increase in total tumor burden within 6 months (27)]. The diagnostic criteria for benign lesions were as follows: i) Histopathological confirmation; or ii) stability in size (no change) during ≥6 months of follow-up. A total of 197 patients (128 with metastases and 69 with benign lesions) were included to develop and validate the models (Fig. 1).

^{18}F-FDG PET/CT procedure. In the present study, PET/CT imaging was performed using a Discovery MI scanner (GE Healthcare). All patients received an intravenous injection of ^{18}F-FDG (4.2 MBq/kg), and imaging was conducted ~60 min post-injection. Prior to the examination, patients were required to fast for ≥6 h and to maintain blood glucose levels at <11 mmol/l. Initially, unenhanced CT images were acquired with the following parameters: 120 kV, 80 mAsec and a slice thickness of 5 mm, covering the region from the skull vertex to the mid-femur during tidal breathing. Subsequently, dedicated full-ring PET images were obtained from the mid-thigh to the vertex of the head during shallow breathing. Image reconstruction was performed using an ordered-subset expectation maximization algorithm with CT-based attenuation correction.

^{18}F-FDG PET/CT image analysis. Two nuclear medicine radiologists with 4 and 6 years of PET/CT diagnostic experience, respectively, independently reviewed the PET/CT images. Disagreements between the two radiologists were settled by consensus. On the CT component, the following adrenal nodule characteristics were assessed: i) Short diameter (SD) and LD; ii) location (left or right); iii) homogeneity (homogeneous or heterogeneous); iv) unenhanced CT value, measured by manually placing a region of interest (ROI) covering two-thirds of the largest transverse lesion section while avoiding adjacent fat tissue. In addition, ROI measurements excluded areas with calcification, hemorrhagic components, cystic degeneration or necrosis. On the PET component, the maximum standardized uptake value (SUV_{max}) was measured by drawing a circular-oval ROI encompassing the entire adrenal nodule and primary lung cancer, carefully avoiding adjacent FDG-avid structures. For reference, an additional ROI was placed in the right posterior superior liver segment. The following metabolic ratios were calculated: Adrenal-to-liver SUV_{max} ratio ($SUR_{adrenal/liver}$) and lung-to-liver SUV_{max} ratio ($SUR_{lung/liver}$). Therefore, six key features were analyzed for each case: i) Morphological characteristics: Size (SD and LD), location, homogeneity and unenhanced CT value; and ii) metabolic parameters: Adrenal nodules [$SUV_{max(adrenal}$ and $SUR_{adrenal/liver}$] and lung cancer ($SUV_{max(lung)}$ and $SUR_{lung/liver}$).

Statistical analysis and model development. In the present study, the models were constructed using an SVM with a linear kernel function and a regularization parameter (C) set to 1. To enhance model interpretability, a single feature from either the metabolic or size features of adrenal lesions or the metabolic features of lung cancer was iteratively selected, combining it with other feature types to build each model. Using stratified random sampling, the study cohort was divided into training (n=148; 96 metastases and 52 benign lesions) and validation (n=49; 32 metastases and 17

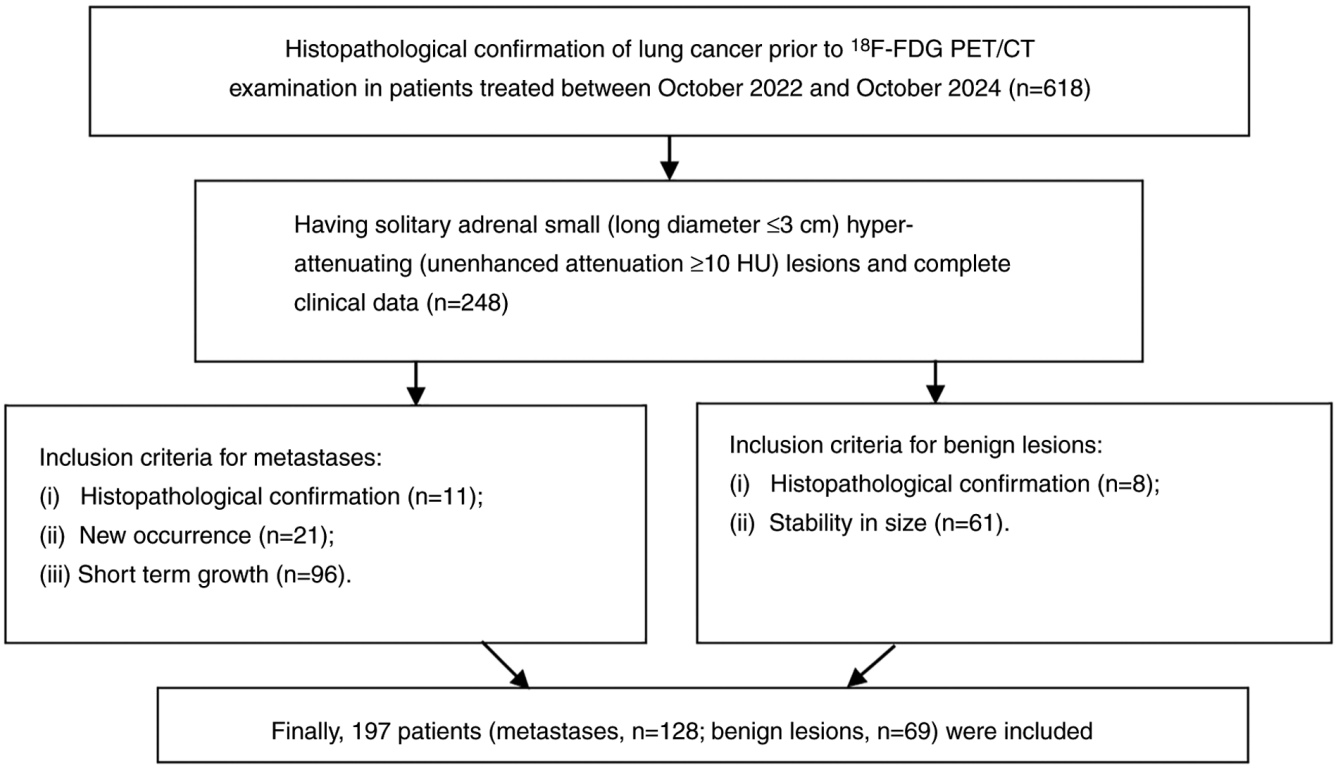

Figure 1. Flowchart illustrating the patient selection process, along with the criteria for inclusion and exclusion. FDG, fluorodeoxyglucose; PET/CT, positron emission tomography/computed tomography.

benign lesions) subsets maintaining a 3:1 allocation ratio. To mitigate sampling bias, this sampling process was repeated 1,000 times. During this process, the area under the receiver operating characteristic curve (AUC) values and accuracies of the models in the validation subsets were used to evaluate their performance. To assess whether the classification accuracy exceeded chance level, a null distribution of accuracies was generated by randomly shuffling the metastatic status labels of adrenal lesions during classifier training, thereby eliminating any predictive information. The P-value was calculated by comparing the actual classification accuracy (derived from correctly labeled data) against the null distribution, defined as the proportion of null accuracies equal to or greater than the observed accuracy (28). Permutation tests were conducted for the best-performing SVM model (namely the models with the highest accuracy). To further evaluate whether SVM was the optimal method for metastasis prediction, its performance was compared with random forest and k-nearest neighbor (KNN) classifiers. Each algorithm was run 1,000 times under identical conditions to ensure comparability, and the distributions of accuracy and AUC were analyzed. For the random forest model, five decision trees were used, with a minimum tree depth of 1 and the number of features per tree set to the square root of the total feature count. For KNN, k was set at 5. To enhance clinical applicability, the model was simplified by scoring features based on their weights and the distribution of continuous variables. The final risk score was computed as the sum of each feature's score multiplied by its mean weight. All analyses were performed using Python (version 3.12; Python Software Foundation). The AUC and accuracy of different models were compared using the Kruskal-Wallis test with Dunn's post hoc test. $P<0.05$ was considered to indicate a statistically significant difference.

Results

Clinical characteristics and PET/CT features. The clinical characteristics of patients in both cohorts are summarized in Table I. The retrospective dataset comprised 197 patients (age range, 28-85 years; males, 126; females, 71), including 128 metastatic lesions and 69 benign adrenal lesions. Among the lung cancer cases, adenocarcinoma represented the predominant histological subtype (134/197, 68.0%), followed by squamous cell carcinoma (48/197, 24.4%). Other histological variants included adenosquamous carcinoma (7/197, 3.6%), large cell carcinoma (4/197, 2.0%), sarcomatoid carcinoma (3/197, 1.5%) and pleomorphic carcinoma (1/197, 0.5%). Table II summarizes six key PET/CT features for both cohorts, including size (SD and LD), metabolism ($SUV_{max(adrenal)}$ and $SUR_{adrenal/liver}$), unenhanced CT value, location and homogeneity of adrenal nodules, and metabolism of lung cancer ($SUV_{max(lung)}$ and $SUR_{lung/liver}$).

Comparison of different models. A total of eight distinct SVM models were developed in the present study, with their respective feature compositions detailed in Table III. For each model, 1,000 iterations of sampling were performed to ensure robust statistical evaluation. Model 1 emerged as the top-performing model, demonstrating superior performance across multiple metrics, including i) AUC: Maximum, 1.000; mean, 0.913; and minimum, 0.770; and ii) accuracy: Maximum, 98.0% (95% CI, 93.9-100%); mean, 84.3% (95% CI, 69.4-91.8%); and

Table I. Clinical characteristics of patients.

Characteristics	Distribution
Sex, n	
Male	126
Female	71
Age, years	
Range	28-85
Mean ± standard deviation	62.71±8.99
Median	63
Histological subtype of lung cancer, n	
Adenocarcinoma	134
Squamous cell carcinoma	48
Other types	15
Adenosquamous carcinoma	7
Large cell carcinoma	4
Sarcomatoid carcinoma	3
Pleomorphic carcinoma	1
Group, n	
Metastases	128
Benign lesions	69

minimum, 71.4% (95% CI, 57.1-83.7%) (Fig. 2). Permutation tests for Model 1 yielded statistically significant results (P<0.001 for the highest-accuracy iteration; P=0.004 for the lowest-accuracy iteration) (Fig. 3). To validate the predictive superiority of SVM, its performance was compared against identically configured random forest and KNN models. SVM significantly outperformed both alternatives in terms of accuracy (both P<0.001) and AUC (both P<0.001) (Fig. 4).

Feature weights of the best model. Table IV presents the ^{18}F-FDG PET/CT feature weights of Model 1. The mean absolute value of weights and the mean of weight were calculated as follows:

$$\text{Mean absolute value of weight}=\frac{|W_1|+|W_2|+\cdots+|W_{1000}|}{1000}$$

$$\text{Mean of weight}=\frac{W_1+W_2+\cdots+W_{1000}}{1000}$$

The mean absolute weight reflects each feature's relative importance in the model. A positive mean weight indicates a positive association with metastases, whereas a negative value suggests an inverse association. Key findings regarding feature importance and association included: i) Homogeneity of adrenal lesions had the lowest mean absolute value of weight; ii) $SUV_{max(adrenal)}$ had the highest mean absolute value of weight; iii) homogeneity and location of adrenal lesions were negatively correlated with metastases; and iv) $SUV_{max(adrenal)}$, $SUV_{max(lung)}$, unenhanced CT value and LD were positively correlated with metastases.

Adrenal metastasis scoring rule. Fig. 5 displays the distributions of $SUV_{max(adrenal)}$, $SUV_{max(lung)}$, LD and unenhanced CT value. To facilitate subsequent model simplification, each continuous variable was categorized using thresholds derived from the approximate mean values of the metastatic and benign groups. The variables were categorized as follows: $SUV_{max(adrenal)}$ was separated into <3, 3-5 and ≥5 g/m; $SUV_{max(lung)}$ was separated into <7.5, 7.5-10 and ≥10 g/m; LD was separated into <1.35, 1.35-1.75 and ≥1.75 cm; and unenhanced CT value was separated into <30, 30-35 and ≥35 HU. The mean weights were used as feature coefficients for scoring. Table V presents the detailed scoring system based on these distributions and coefficients, whereby each factor was assigned a score according to predetermined thresholds, and the final risk score was calculated as the sum of each factor's score multiplied by its mean weighting coefficient. Fig. 6 illustrates the final score distribution. The final scores were as follows: 56.5% (39/69) of adrenal benign lesions scored <5, whereas only 7.03% (9/128) of adrenal metastases scored <5. Furthermore, only 5.80% (4/69) of the final scores of benign lesions were >6.5, but 68.8% (88/128) of those for metastases were >6.5. Finally, the following diagnostic criteria were established: Adrenal nodules with scores <5 were benign; those with scores >6.5 were metastatic; and those with scores 5-6.5 were suspicious for metastasis.

Discussion

The adrenal gland is a frequent site of metastasis, particularly in patients with lung cancer (29). However, differentiating metastatic from benign adrenal lesions in these patients remains clinically challenging due to the overlapping prevalence of neoplastic and non-neoplastic adrenal masses (30,31). Compared with conventional CT or MRI, ^{18}F-FDG PET/CT offers distinct advantages by providing both functional metabolic data and anatomical information. This synergistic capability has verified the use of PET/CT as an invaluable tool in the evaluation of primary lung cancer and its metastatic spread, particularly in characterizing rare soft-tissue masses (32) and indeterminate solitary hyperattenuating adrenal lesions (33). In the current study, an SVM model was developed using ^{18}F-FDG PET/CT parameters that demonstrated superior performance to both KNN and random forest algorithms, achieving high predictive accuracy (AUC=0.913) for identifying adrenal metastases. Among the predictive features, $SUV_{max(adrenal)}$ emerged as the most significant contributor, with a mean absolute weight of 1.25 in the model. To enhance clinical applicability, the model was subsequently simplified into a practical scoring system. This streamlined approach maintains diagnostic accuracy while facilitating implementation in routine clinical practice.

Recent studies have demonstrated the promising diagnostic performance of ^{18}F-FDG PET/CT in detecting adrenal metastases in patients with lung cancer (23,34,35). Evans *et al* (34) reported that SUV_{max} exhibited marked diagnostic efficacy, with a mean sensitivity of 91%, specificity of 81% and accuracy of 83% for identifying adrenal metastases. Similarly, Orzechowski *et al* (23) revealed that SUVs provided reliable assessment of adrenal metastases, achieving an AUC of 0.83. Notably, Kim *et al* (35) demonstrated even higher diagnostic accuracy using $SUR_{adrenal/liver}$ (AUC, 0.933; sensitivity, 87%; specificity, 100%) in patients

Table II. Positron emission tomography/CT features of patients.

Features	Metastases (n=128)	Benign lesions (n=69)
Size of adrenal lesions, cm[a]		
SD	1.39±0.41	1.23±0.33
LD	1.81±0.51	1.52±0.48
Metabolism of adrenal lesions[a]		
$SUV_{max(adrenal)}$, g/m	5.60±2.24	3.03±0.91
$SUR_{adrenal/liver}$	1.74±0.69	1.02±0.26
Unenhanced CT value of adrenal lesions[a]	35.97±6.40	28.99±6.48
Location of adrenal lesions, n		
Left	83	48
Right	45	21
Homogeneity of adrenal lesions, n		
Homogeneous	108	54
Heterogeneous	20	15
Metabolism of lung cancer[a]		
$SUV_{max(lung)}$, g/m	10.50±4.33	6.55±2.92
$SUR_{lung/liver}$	3.27±1.35	2.25±1.06

[a]Data are presented as the mean ± standard deviation. CT, computed tomography; SD, short diameter; LD, long diameter; SUV_{max}, maximum standard uptake value; $SUR_{adrenal/liver}$, adrenal-to-liver SUV_{max} ratio; $SUR_{lung/liver}$, lung-to-liver SUV_{max} ratio.

Table III. Combination of different types of features.

Model number	Metabolism of adrenal lesions	Size of adrenal lesions	Metabolism of lung cancers	Unenhanced CT value of adrenal lesions	Location of adrenal lesions	Homogeneity of adrenal lesions
1	$SUV_{max(adrenal)}$	LD	$SUV_{max(lung)}$	Hounsfield unit	Right/left	Yes/no
2	$SUV_{max(adrenal)}$	LD	$SUR_{lung/liver}$	Hounsfield unit	Right/left	Yes/no
3	$SUV_{max(adrenal)}$	SD	$SUV_{max(lung)}$	Hounsfield unit	Right/left	Yes/no
4	$SUV_{max(adrenal)}$	SD	$SUR_{lung/liver}$	Hounsfield unit	Right/left	Yes/no
5	$SUR_{adrenal/liver}$	LD	$SUV_{max(lung)}$	Hounsfield unit	Right/left	Yes/no
6	$SUR_{adrenal/liver}$	LD	$SUR_{lung/liver}$	Hounsfield unit	Right/left	Yes/no
7	$SUR_{adrenal/liver}$	SD	$SUV_{max(lung)}$	Hounsfield unit	Right/left	Yes/no
8	$SUR_{adrenal/liver}$	SD	$SUR_{lung/liver}$	Hounsfield unit	Right/left	Yes/no

CT, computed tomography; SD, short diameter; LD long diameter, SUV_{max}, maximum standard uptake value; $SUR_{adrenal/liver}$, adrenal-to-liver SUV_{max} ratio; $SUR_{lung/liver}$, lung-to-liver SUV_{max} ratio.

with non-small cell lung cancer. However, the small sample size of this previous study (n=24 patients with suspicious adrenal masses) may limit the generalizability of its findings. A critical limitation common to these studies is their reliance on single metabolic parameters for metastasis prediction. As established in the literature, single-parameter approaches have inherent constraints: i) They often demonstrate suboptimal diagnostic performance, and ii) they cannot comprehensively characterize the multifaceted nature of adrenal metastases. To enhance diagnostic accuracy, recent studies have explored multi-parameter approaches for predicting adrenal metastases (9,36,37). Brady *et al* (9) demonstrated that combining SUV_{max} >3.1 with mean attenuation >10 HU achieved excellent diagnostic performance (sensitivity, 97.3%; specificity, 86.2%; accuracy, 90.5%). Similarly, Cho *et al* (36) reported that an adrenal-to-liver SUV_{max} ratio >1.3 combined with HU >18 yielded a sensitivity of 97.7%, a specificity of 81.2% and an accuracy of 93.4% in patients with lung cancer. Notably, Lu *et al* (37) revealed that integrating PET and CT features achieved optimal performance (sensitivity, 100%; specificity, 98%; accuracy, 99%). These findings collectively suggest that combining PET and CT parameters may provide superior predictive value for adrenal metastases in clinical practice. However, most previous studies included adrenal masses of all sizes, limiting their applicability to solitary small hyperattenuating lesions, a particularly challenging

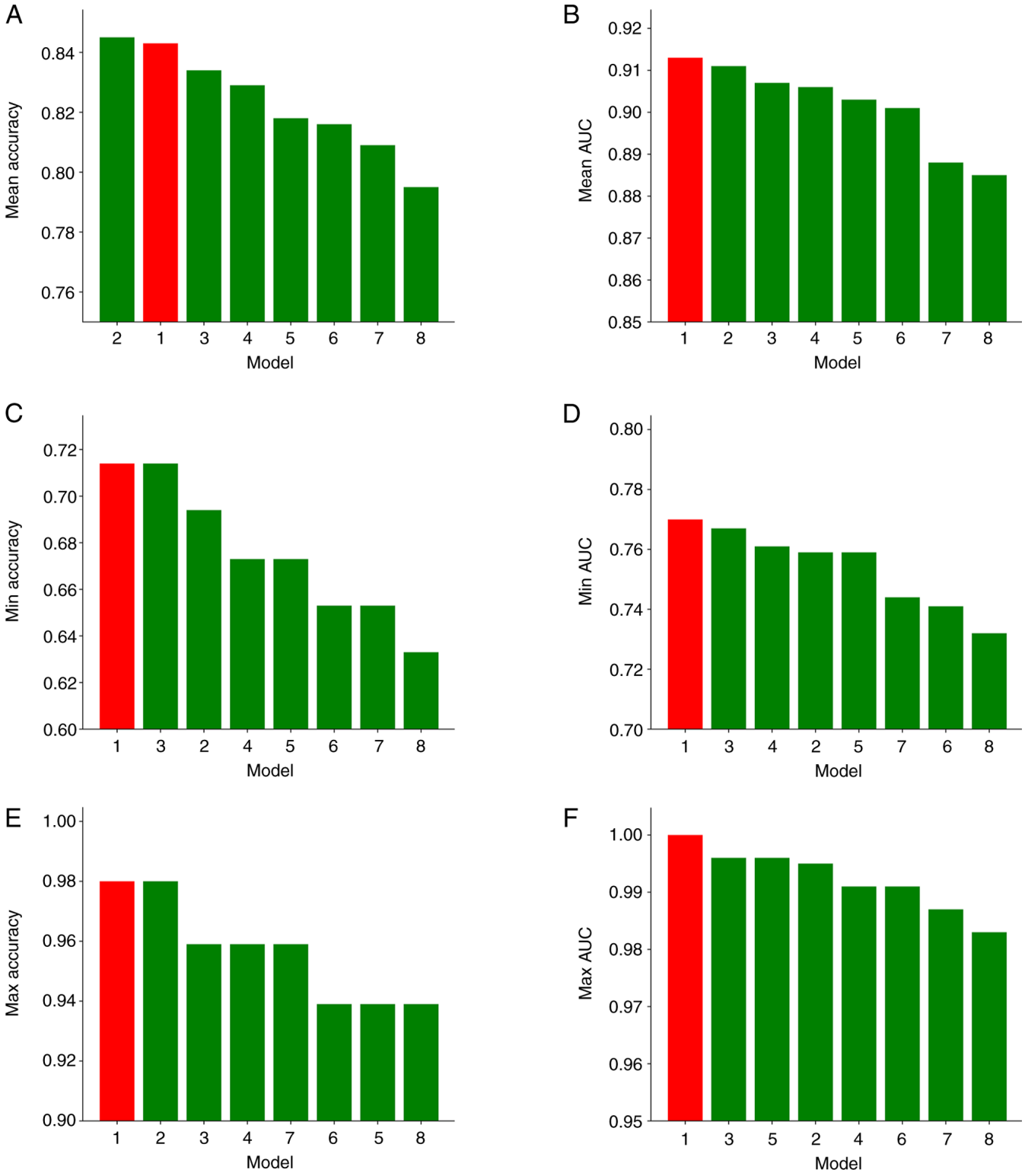

Figure 2. Comparison of different models. (A) Model 1 exhibited the second highest values for mean accuracy. (B) Model 1 exhibited the highest values for mean AUC. (C) For min accuracy, models 1 and 3 were tied for the highest values. (D) Model 1 exhibited the highest values for min AUC. (E) For max accuracy, models 1 and 2 were tied for the highest values. (F) Model 1 exhibited the highest values for max AUC. AUC, area under the receiver operating characteristic curve; Max, maximum; Min, minimum.

diagnostic scenario where false-negative results frequently occur (1,19,34,35). To address this limitation, the current study developed an SVM model incorporating multiple clinically relevant PET and CT features specifically for small adrenal lesions. The model demonstrated robust performance, with a mean AUC of 0.913 and accuracy of 84.3%. Notably, the clinical utility of the model was enhanced by: i) Improving interpretability through feature importance analysis, and ii) developing a simplified scoring system to facilitate clinical staging decisions in patients with lung cancer.

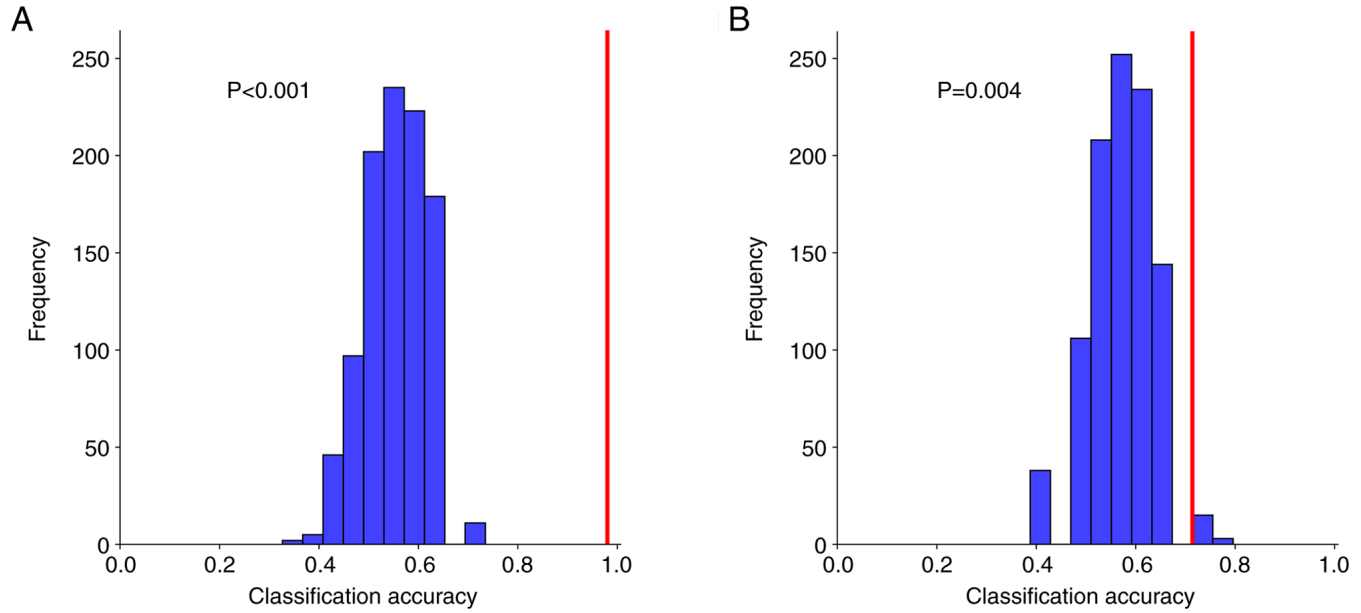

Figure 3. Permutation tests for the SVM results of model 1 with the highest and lowest accuracy. (A) Permutation test for the SVM result of model 1 with the highest accuracy (98.0%; P<0.001). (B) Permutation test for the SVM result of model 1 with the lowest accuracy (71.4%; P=0.004). Both of the true classification accuracies of model 1 with highest and lowest accuracy (red bar) were significantly higher than those after random sampling, grouping and shuffling of labels (blue bar). SVM, support vector machine.

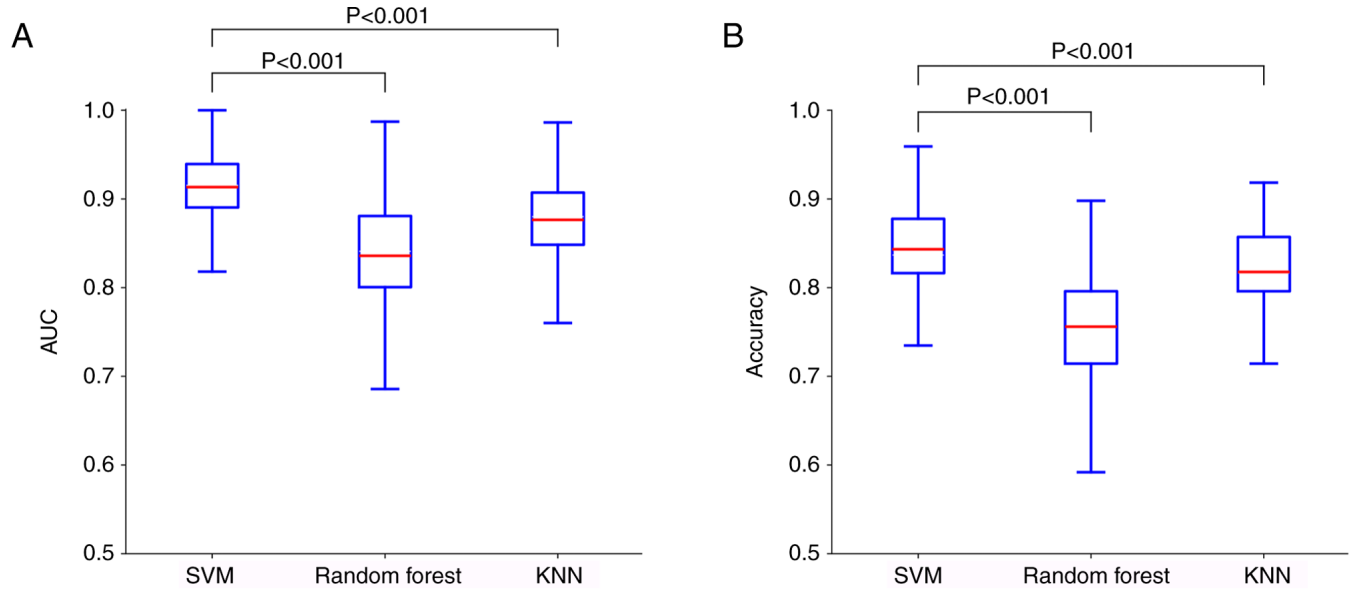

Figure 4. Distribution and comparison of AUC and accuracy of the SVM, random forest and KNN. (A) The AUC of the SVM was significantly higher than those of the random forest and KNN methods (both P<0.001). (B) The accuracy of the SVM was also significantly higher than those of the random forest and KNN methods (both P<0.001). AUC, area under the receiver operating characteristic curve; KNN, k-nearest neighbor; SVM, support vector machine.

In the current linear SVM model, feature importance was quantified by the mean absolute weight, where higher values indicated stronger predictive contributions for adrenal metastases. Among all features, $SUV_{max(adrenal)}$ demonstrated the weight of highest importance. This finding aligns with established literature demonstrating the diagnostic value of metabolic parameters such as SUV_{max} in detecting adrenal metastases (18,20,38). Koopman *et al* (38) reported significantly higher SUV_{max} values in metastatic vs. benign adrenal lesions, with optimal diagnostic performance (96% sensitivity and specificity) at a cutoff of 3.7 for detecting metastatic adrenal lesions in patients with lung cancer. The biological basis for this observation relates to SUV being a surrogate for Km (the absolute metabolic rate of glucose consumption). Malignant lesions typically exhibit elevated Km values due to their characteristically increased glucose metabolism (39). The prominent weight of $SUV_{max(adrenal)}$ in the present model substantiates its critical diagnostic role. Additionally, $SUV_{max(lung)}$ showed considerable predictive weight, suggesting that higher metabolic activity in primary lung tumors may be

Table IV. Weight of features for the best model.

Characteristics	Mean weight	Mean absolute value of weight
Homogeneity of adrenal lesions	-0.177±0.097	0.179±0.094
Location of adrenal lesions	-0.146±0.158	0.183±0.115
Unenhanced CT value of adrenal lesions	0.702±0.114	0.702±0.114
LD of adrenal lesions	0.443±0.112	0.443±0.112
$SUV_{max(adrenal)}$	1.247±0.170	1.247±0.170
$SUV_{max(lung)}$	0.709±0.137	0.709±0.137

CT, computed tomography; LD, long diameter; SUV_{max}, maximum standard uptake value.

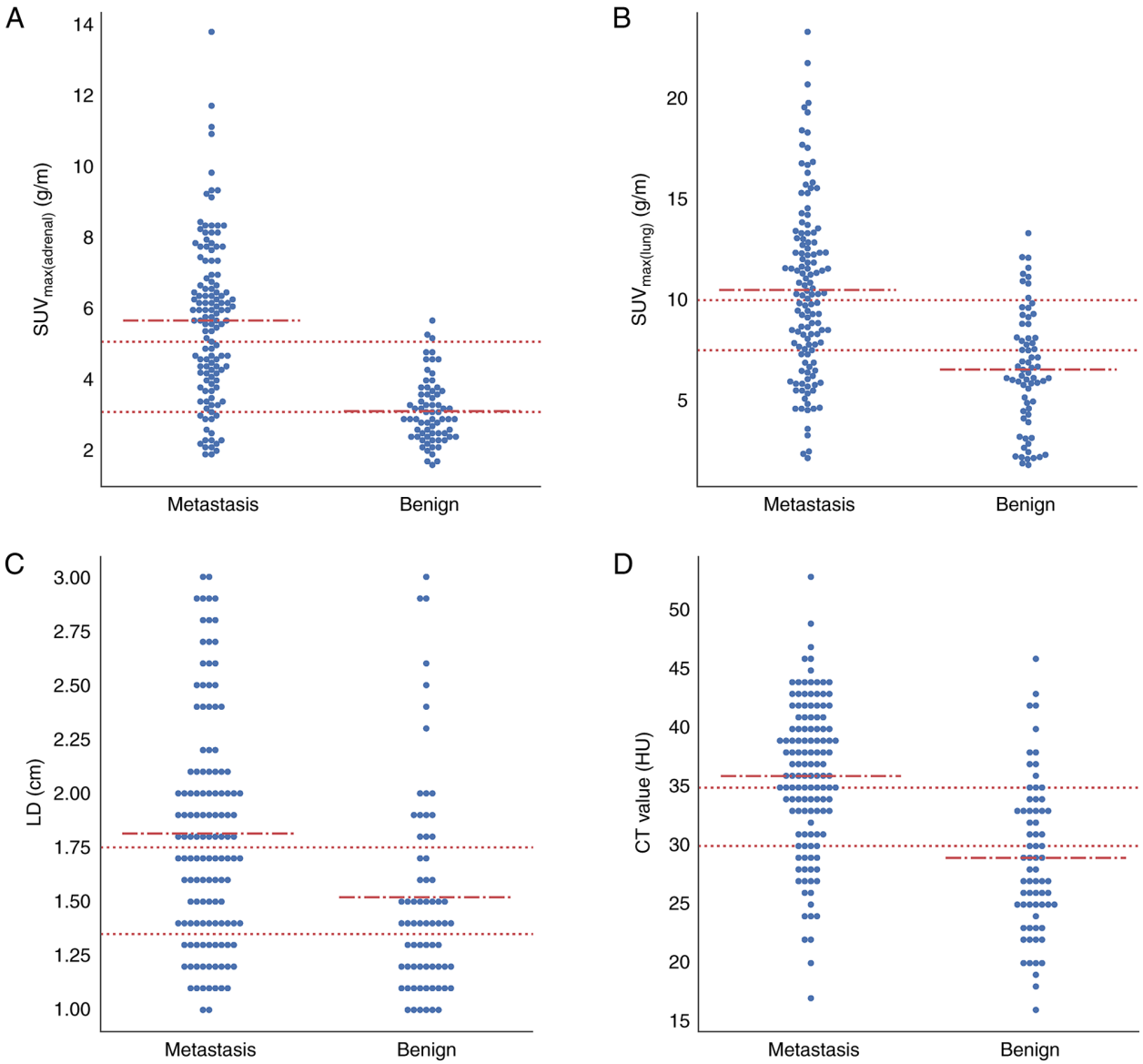

Figure 5. Distribution of $SUV_{max(adrenal)}$, $SUV_{max(lung)}$, LD and CT values. (A) $SUV_{max(adrenal)}$ was separated into <3, 3-5 and ≥5 g/m. (B) $SUV_{max(lung)}$ was separated into <7.5, 7.5-10 and ≥10 g/m. (C) LD was separated into <1.35, 1.35-1.75 and ≥1.75 cm. (D) CT value was separated into <30 HU, 30-35 HU and ≥35 HU. SUV_{max}, maximum standardized uptake value; LD, long diameter; CT, computed tomography.

associated with greater metastatic potential. This association has been previously documented (40,41): Zhang *et al* (40) identified primary tumor SUV_{max} as a significant predictor of lymph node metastasis and Zhu *et al* (41) similarly reported that elevated SUV_{max} in non-small cell lung cancer is associated with increased metastatic risk.

Table V. Final scoring rules for predicting adrenal metastases.

	SUV_{max} (adrenal), g/m			SUV_{max} (lung), g/m			LD, cm			Unenhanced CT value, HU			Location		Homogeneity	
Factor	<3	3-5	≥5	<7.5	7.5-10	≥10	<1.35	1.35-1.75	≥1.75	<30	30-35	≥35	L	R	Yes	No
Score	1	2	3	1	2	3	1	2	3	1	2	3	0	1	0	1
Coefficient		1.25			0.71			0.44			0.70			-0.15		-0.18

SUV_{max}, maximum standard uptake value; LD, long diameter; CT, computed tomography; L, left; R, right.

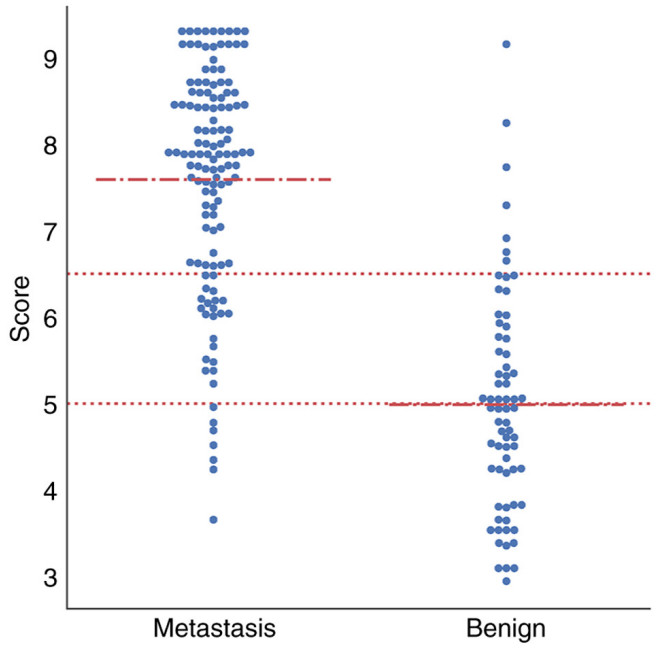

Figure 6. Score distribution of adrenal benign and metastatic lesions. The red dashed lines represented the thresholds of score. The difference of scores between benign and metastatic lesions was more apparent after being simplified.

Multiple studies have established that while PET features may yield false-negative results in cases of micro-metastases, integrated PET/CT demonstrates superior diagnostic accuracy for detecting adrenal metastases compared with PET or CT alone (1,36,37). This underscores the importance of incorporating CT features to enhance diagnostic performance. The present analysis revealed that unenhanced CT value served a corrective function in the model. This finding aligns with the existing literature demonstrating that adrenal metastases typically exhibit higher attenuation values than benign lesions (36,42). For example, Cho *et al* (36) reported significant differences in unenhanced CT values between metastatic (29±8 HU) and non-metastatic (9±13 HU) adrenal lesions, with a HU threshold of >18 achieving an AUC of 0.925 (sensitivity, 86.7%; specificity, 81.2%; accuracy, 85.2%). Chen *et al* (43) subsequently identified a pre-contrast CT value of >30 HU as an independent predictor of metastases (AUC, 0.766), a potentially more robust criterion. The underlying pathophysiology relates to adipose tissue content, which serves as a key diagnostic marker for adenomas (42). The present results corroborate these established attenuation patterns. Furthermore, lesion size emerged as another significant CT parameter, with metastases typically demonstrating larger dimensions than benign lesions, which was consistent with previous research (23,34). Evans *et al* (34) documented markedly larger metastatic lesions (mean, 3.0 cm; range, 1.0-9.2 cm) vs. benign lesions (mean, 1.9 cm; range, 0.7-5.3 cm). In addition, Orzechowski *et al* (23) reported that a size threshold of >25 mm yielded 83.33% sensitivity, 83.64% specificity and 83.49% accuracy for metastasis detection.

The location and homogeneity of adrenal lesions also contributed to the present predictive model. It was observed that adrenal metastases demonstrated a left-sided predominance and more heterogeneous appearance, consistent with prior studies (22,43). However, the mean absolute weights for these features were markedly lower than those of the four primary parameters [$SUV_{max(adrenal)}$, $SUV_{max(lung)}$, unenhanced CT value and size].

The current study has several limitations that should be acknowledged. First, the subjective interpretation of certain imaging features (particularly lesion homogeneity) may vary between radiologists, with more experienced practitioners likely demonstrating greater diagnostic accuracy. Future incorporation of computer-assisted feature evaluation could enhance measurement reproducibility and model stability. Second, as a single-center study with a relatively small sample size, the findings may be specific to the particular PET system, acquisition protocol and reconstruction algorithm employed. Multi-center validation studies with larger cohorts are needed to establish the generalizability of the coefficients across different imaging platforms. Third, in the 21 patients with interval development of adrenal metastases, the SUV_{max} of the primary lung cancer may have changed due to tumor progression or recurrence. Future studies with larger cohorts are warranted to systematically assess whether the change in SUV_{max} has diagnostic value in differentiating adrenal metastases and whether it affects the performance of the model. Fourth, it is notable that some of the patients with lung cancer included in the present study also had comorbid fatty liver. Hepatic steatosis in patients with cancer may alter metabolic activity and influence 18F-FDG uptake (44). Although the SUR was not a parameter in the final model, further corrections should be considered in future studies when the liver is used as a comparator for PET-CT scans in patients with lung cancer.

In conclusion, the present study describes the development of an interpretable SVM model using ^{18}F-FDG PET/CT

features to predict adrenal metastases in patients with lung cancer. The model identified $SUV_{max(adrenal)}$ as the most significant predictor, followed by $SUV_{max(lung)}$, unenhanced CT value, size, homogeneity and location. For clinical implementation, the SVM model was simplified into a practical scoring system that may facilitate staging decisions for patients with lung cancer.

Acknowledgements

Not applicable.

Funding

This study received funding from the Tangshan City Key Research and Development Program (grant no. 24150216C).

Availability of data and materials

The data generated in the present study may be requested from the corresponding author.

Authors' contributions

LZ, HC, WZ, JL, YL and LC designed the study. ZL, CH and ZW collected the patient images, performed the statistical analysis and wrote the manuscript. CL, LJ and LY critically reviewed the manuscript. All authors contributed to the article and have read and approved the final manuscript. CL and ZL confirm the authenticity of all the raw data.

Ethics approval and consent to participate

The present study was approved by the Medical Ethics Committee of Tangshan People's Hospital (Tangshan, China). The requirement for informed consent was waived due to the retrospective nature of the study, and the study was performed in accordance with The Declaration of Helsinki.

Patient consent for publication

Not applicable.

Competing interests

The authors declare that they have no competing interests.

References

1. Bray F, Laversanne M, Sung H, Ferlay J, Siegel RL, Soerjomataram I and Jemal A: Global cancer statistics 2022: GLOBOCAN estimates of incidence and mortality worldwide for 36 cancers in 185 countries. CA Cancer J Clin 74: 229-263, 2024.
2. Besse B, Adjei A, Baas P, Meldgaard P, Nicolson M, Paz-Ares L, Reck M, Smit EF, Syrigos K, Stahel R, *et al*: 2nd ESMO consensus conference on lung cancer: Non-small-cell lung cancer first-line/second and further lines of treatment in advanced disease. Ann Oncol 25: 1475-1484, 2014.
3. Burt M, Heelan RT, Coit D, McCormack PM, Bains MS, Martini N, Rusch V and Ginsberg RJ: Prospective evaluation of unilateral adrenal masses in patients with operable non-small-cell lung cancer. Impact of magnetic resonance imaging. J Thorac Cardiovasc Surg 107: 584-599, 1994.
4. Kawai N, Tozawa K, Yasui T, Moritoki Y, Sasaki H, Yano M, Fujii Y and Kohri K: Laparoscopic adrenalectomy for solitary adrenal metastasis from lung cancer. JSLS 18: e2014.00062, 2014.
5. Porte HL, Roumilhac D, Graziana JP, Eraldi L, Cordonier C, Puech P and Wurtz AJ: Adrenalectomy for a solitary adrenal metastasis from lung cancer. Ann Thorac Surg 65: 331-335, 1998.
6. Gao XL, Zhang KW, Tang MB, Zhang KJ, Fang LN and Liu W: Pooled analysis for surgical treatment for isolated adrenal metastasis and non-small cell lung cancer. Interact Cardiovasc Thorac Surg 24: 1-7, 2017.
7. Holy R, Piroth M, Pinkawa M and Eble MJ: Stereotactic body radiation therapy (SBRT) for treatment of adrenal gland metastases from non-small cell lung cancer. Strahlenther Onkol 187: 245-251, 2011.
8. Cao L, Yang H, Yao D, Cai H, Wu H, Yu Y, Zhu L, Xu W, Liu Y and Li J: Clinical-imaging-radiomic nomogram based on unenhanced CT effectively predicts adrenal metastases in patients with lung cancer with small hyperattenuating adrenal incidentalomas. Oncol Lett 28: 340, 2024.
9. Brady MJ, Thomas J, Wong TZ, Franklin KM, Ho LM and Paulson EK: Adrenal nodules at FDG PET/CT in patients known to have or suspected of having lung cancer: A proposal for an efficient diagnostic algorithm. Radiology 250: 523-530, 2009.
10. Zeiger MA, Siegelman SS and Hamrahian AH: Medical and surgical evaluation and treatment of adrenal incidentalomas. J Clin Endocrinol Metab 96: 2004-2015, 2011.
11. Cao L, Yang H, Wu H, Zhong H, Cai H, Yu Y, Zhu L, Liu Y and Li J: Adrenal indeterminate nodules: CT-based radiomics analysis of different machine learning models for predicting adrenal metastases in lung cancer patients. Front Oncol 14: 1411214, 2024.
12. Caoili EM, Korobkin M, Francis IR, Cohan RH, Platt JF, Dunnick NR and Raghupathi KI: Adrenal masses: Characterization with combined unenhanced and delayed enhanced CT. Radiology 222: 629-633, 2002.
13. Fujiyoshi F, Nakajo M, Fukukura Y and Tsuchimochi S: Characterization of adrenal tumors by chemical shift fast low-angle shot MR imaging: Comparison of four methods of quantitative evaluation. AJR Am J Roentgenol 180: 1649-1657, 2003.
14. Mayo-Smith WW, Song JH, Boland GL, Francis IR, Israel GM, Mazzaglia PJ, Berland LL and Pandharipande PV: Management of incidental adrenal masses: A white paper of the ACR incidental findings committee. J Am Coll Radiol 14: 1038-1044, 2017.
15. Haider MA, Ghai S, Jhaveri K and Lockwood G: Chemical shift MR imaging of hyperattenuating (>10 HU) adrenal masses: Does it still have a role? Radiology 231: 711-716, 2004.
16. Koo HJ, Choi HJ, Kim HJ, Kim SO and Cho KS: The value of 15-minute delayed contrast-enhanced CT to differentiate hyperattenuating adrenal masses compared with chemical shift MR imaging. Eur Radiol 24: 1410-1420, 2014.
17. Hsiao R, Chow A, Kluijfhout WP, Bongers PJ, Verzijl R, Metser U, Veit-Haibach P and Pasternak JD: The clinical consequences of functional adrenal uptake in the absence of cross-sectional mass on FDG-PET/CT in oncology patients. Langenbecks Arch Surg 407: 1677-1684, 2022.
18. Arikan AE, Makay O, Teksoz S, Vatansever S, Alptekin H, Albeniz G, Demir A, Ozpek A and Tunca F: Efficacy of PET-CT in the prediction of metastatic adrenal masses that are detected on follow-up of the patients with prior nonadrenal malignancy: A nationwide multicenter case-control study. Medicine (Baltimore) 101: e30214, 2022.
19. Lang BH, Cowling BJ, Li JY, Wong KP and Wan KY: High false positivity in positron emission tomography is a potential diagnostic pitfall in patients with suspected adrenal metastasis. World J Surg 39: 1902-1908, 2015.
20. Detterbeck FC, Woodard GA, Bader AS, Dacic S, Grant MJ, Park HS and Tanoue LT: The proposed ninth edition TNM classification of lung cancer. Chest 166: 882-895, 2024.
21. Vos EL, Grewal RK, Russo AE, Reidy-Lagunes D, Untch BR, Gavane SC, Boucai L, Geer E, Gopalan A, Chou JF, *et al*: Predicting malignancy in patients with adrenal tumors using ^{18}F-FDG-PET/CT SUVmax. J Surg Oncol 122: 1821-1826, 2020.
22. Xu B, Gao J, Cui L, Wang H, Guan Z, Yao S, Shen Z and Tian J: Characterization of adrenal metastatic cancer using FDG PET/CT. Neoplasma 59: 92-99, 2012.

23. Orzechowski S, Gnass M, Czyżewski D, Wojtacha J, Sudoł B, Pankowski J, Zajęcki W, Ćmiel A, Zieliński M and Szlubowski A: Ultrasound predictors of left adrenal metastasis in patients with lung cancer: A comparison of computed tomography, positron emission tomography-computed tomography, and endoscopic ultrasound using ultrasound bronchoscope. Pol Arch Intern Med 132: 16127, 2022.
24. Noble WS: What is a support vector machine? Nat Biotechnol 24: 1565-1567, 2006.
25. Yin G, Song Y, Li X, Zhu L, Su Q, Dai D and Xu W: Prediction of mediastinal lymph node metastasis based on ^{18}F-FDG PET/CT imaging using support vector machine in non-small cell lung cancer. Eur Radiol 31: 3983-3992, 2021.
26. Zhang R, Zhu L, Cai Z, Jiang W, Li J, Yang C, Yu C, Jiang B, Wang W, Xu W, *et al*: Potential feature exploration and model development based on 18F-FDG PET/CT images for differentiating benign and malignant lung lesions. Eur J Radiol 121: 108735, 2019.
27. Nishino M, Jagannathan JP, Ramaiya NH and Van den Abbeele AD: Revised RECIST guideline version 1.1: What oncologists want to know and what radiologists need to know. AJR Am J Roentgenol 195: 281-289, 2010.
28. Liang M, Su Q, Mouraux A and Iannetti GD: Spatial patterns of brain activity preferentially reflecting transient pain and stimulus intensity. Cereb Cortex 29: 2211-2227, 2019.
29. Mendez AM, Petre EN, Ziv E, Ridouani F, Solomon SB, Sotirchos V, Zhao K and Alexander ES: Safety and efficacy of thermal ablation of adrenal metastases secondary to lung cancer. Surg Oncol 55: 102102, 2024.
30. Andersen MB, Bodtger U, Andersen IR, Thorup KS, Ganeshan B and Rasmussen F: Metastases or benign adrenal lesions in patients with histopathological verification of lung cancer: Can CT texture analysis distinguish? Eur J Radiol 138: 109664, 2021.
31. Al Fares HK, Abdullaj S, Gokden N and Menon LP: Incidental, solitary, and unilateral adrenal metastasis as the initial manifestation of lung adenocarcinoma. Cureus 14: e32628, 2022.
32. Hashimoto K, Nishimura S and Akagi M: Lung adenocarcinoma presenting as a soft tissue metastasis to the shoulder: A case report. Medicina (Kaunas) 57: 181, 2021.
33. Lococo F, Patricelli G, Galeone C and Rapicetta C: eComment. Surgery for isolated adrenal metastasis from non-small-cell lung cancer: The role of preoperative PET/CT scan'. Interact Cardiovasc Thorac Surg 24: 7, 2017.
34. Evans PD, Miller CM, Marin D, Stinnett SS, Wong TZ, Paulson EK and Ho LM: FDG-PET/CT characterization of adrenal nodules: Diagnostic accuracy and interreader agreement using quantitative and qualitative methods. Acad Radiol 20: 923-929, 2013.
35. Kim BS, Lee JD and Kang WJ: Differentiation of an adrenal mass in patients with non-small cell lung cancer by means of a normal range of adrenal standardized uptake values on FDG PET/CT. Ann Nucl Med 29: 276-283, 2015.
36. Cho AR, Lim I, Na II, Choe du H, Park JY, Kim BI, Cheon GJ, Choi CW and Lim SM: Evaluation of adrenal masses in lung cancer patients using F-18 FDG PET/CT. Nucl Med Mol Imaging 45: 52-58, 2011.
37. Lu Y, Xie D, Huang W, Gong H and Yu J: 18F-FDG PET/CT in the evaluation of adrenal masses in lung cancer patients. Neoplasma 57: 129-134, 2010.
38. Koopman D, van Dalen JA, Stigt JA, Slump CH, Knollema S and Jager PL: Current generation time-of-flight (18)F-FDG PET/CT provides higher SUVs for normal adrenal glands, while maintaining an accurate characterization of benign and malignant glands. Ann Nucl Med 30: 145-152, 2016.
39. Smith TA: Facilitative glucose transporter expression in human cancer tissue. Br J Biomed Sci 56: 285-292, 1999.
40. Zhang S, Li S, Pei Y, Huang M, Lu F, Zheng Q, Li N and Yang Y: Impact of maximum standardized uptake value of non-small cell lung cancer on detecting lymph node involvement in potential stereotactic body radiotherapy candidates. J Thorac Dis 9: 1023-1031, 2017.
41. Zhu SH, Zhang Y, Yu YH, Fu Z, Kong L, Han DL, Fu L, Yu JM and Li J: FDG PET-CT in non-small cell lung cancer: Relationship between primary tumor FDG uptake and extensional or metastatic potential. Asian Pac J Cancer Prev 14: 2925-2929, 2013.
42. Sherlock M, Scarsbrook A, Abbas A, Fraser S, Limumpornpetch P, Dineen R and Stewart PM: Adrenal incidentaloma. Endocr Rev 41: 775-820, 2020.
43. Chen J, He Y, Zeng X, Zhu S and Li F: Distinguishing between metastatic and benign adrenal masses in patients with extra-adrenal malignancies. Front Endocrinol (Lausanne) 13: 978730, 2022.
44. Ali MA, El-Abd E, Morsi M, El Safwany MM and El-Sayed MZ: The effect of hepatic steatosis on 18F-FDG uptake in PET-CT examinations of cancer Egyptian patients. Eur J Hybrid Imaging 7: 19, 2023.